Stochastic modeling of protein motions within cell membranes

Sharon Khan,[1] Andy M. Reynolds,[1,*] Ian E. G. Morrison,[2] and Richard J. Cherry[2]
[1]*Rothamsted Research, Harpenden, Hertfordshire AL5 2LQ, United Kingdom*
[2]*Department of Biological Sciences, University of Essex, Colchester CO4 3SQ, United Kingdom*
(Received 2 November 2004; published 29 April 2005)

A simple model in which immobilizing events are imposed onto otherwise free Brownian diffusion [R. Metzler and J. Klafter, Phys. Rep. **339**, 1 (2000) and a recent adaptation due to S. Khan and A. M. Reynolds, Physica A **350**, 183 (2005)] is shown to encapsulate the peculiar transport characteristics of individual cell receptors within plasma membranes observed in single-particle tracking (SPT) experiments. These characteristics include the occurrence of normal diffusion; non-Gaussian subdiffusion; confined diffusion; a superdiffusive mode of transport that is not due to flow of the membrane or molecular motor attachment; and the occurrence of transitions between these transport modes. Model predictions are shown to be in close agreement with a reanalysis of existing SPT data.

DOI: 10.1103/PhysRevE.71.041915 PACS number(s): 87.15.Vv, 05.10.Gg, 05.40.Jc, 45.10.Hj

INTRODUCTION

Observations of trajectories of individual proteins in plasma membranes show a variety of types of motion including ordinary Brownian motion, directed motion, and confined and subdiffusion [1–8]. This variety of motion impacts significantly upon the kinetics of reactions among membrane-bound species and serves as a probe of membrane structure [9]. Many mechanisms may be involved, including obstruction by mobile or immobile proteins; transient binding to immobile proteins; confinement by membrane skeletal corrals; binding or obstruction by the extracellular matrix; restrictions to motion imposed by lipid domains; and hydrodynamic interactions ([9] and references therein). These mechanisms have proved difficult to isolate, in large part because some or all of them occur simultaneously and because their relative importance may depend on the protein and the cell type. Transitions between transport modes and non-Gaussian diffusion characteristics have also been observed [9,10]. This calls into question the traditional understanding of protein mobility as the free Brownian diffusion of a limited mobile fraction.

In this paper we show that a simple phenomenological model in which immobilizing events are imposed onto otherwise free Brownian diffusion encapsulates all of the peculiar transport characteristics of individual proteins within plasma membranes and, when combined with a fluctuating force that is colored rather than white, allows for the occurrence of superdiffusivity and confined diffusion. In this model the membrane is regarded as a random array of continuously changing traps [7] with a distribution of energies or escape times so broad that there is no average residence time. The model is shown to account naturally for observed transitions between transport modes without the need to resort to *ad hoc* assumptions about the partitioning of mobile species into different microdomains or an active control mechanism such as transient binding to a cytoskeletal motor [11,12]. Model predictions for mean-square displacements at both short and long times and distributions of incremental displacements are shown to be in close accord with a reanalysis of existing data. This reanalysis also yields identification of a truly superdiffusive transport mode. In contrast with previous observations [13] this form of superdiffusive motion cannot be attributed to flow of the membrane or to molecular motor attachment.

The model is presented in Sec. II. This is followed in Sec. III by comparisons of model predictions with data from single-particle tracking (SPT) experiments. Sec. IV contains a summary.

IMPOSITION OF IMMOBILIZING EVENTS ONTO BROWNIAN MOTION

A particle moving in a fluidlike medium experiences two forces: a frictional force and a fluctuating force $F(t)$ originating from the collisions with the particles of the surrounding medium. When the density of the medium is much less than that of the particle, the fluctuating force can be treated as white noise whereas for dense fluids and for fluids with internal rotational degrees of freedom, it is colored. When correlations persist for a time τ_c, the evolution of the probability density function (PDF) $P(x,t)$ for the displacement x at time t of a Brownian particle is described by the telegraph equation

$$\tau_c \frac{\partial^2 P(x,t)}{\partial t^2} + \frac{\partial P(x,t)}{\partial t} = K \frac{\partial^2 P(x,t)}{\partial x^2}, \tag{1}$$

where K is the mean diffusion coefficient. For times much less than the correlation time scale τ_c, particles travel in straight lines and transport is ballistic, with mean-square particle displacements from the origin evolving according to $\langle x^2 \rangle = Kt^2/\tau_c$. At much later times transport is diffusive, $\langle x^2 \rangle = 2Kt$, and Gaussian. Here, the time scale τ_c for directed motion is not associated exclusively with the effects of inertia, which are widely accepted [14–16] as being irrelevant to

*FAX: +44 (0)1582 760981. Electronic address: andy.reynolds@bbsrc.ac.uk

motions of membrane-bound proteins over times exceeding several nanoseconds. It may be associated with other well-established and dynamically important mechanisms for directed transport; including transit flow of the membrane and attachment to molecular motors.

Predictions from such one-dimensional models can be compared directly with data for the displacements of membrane-bound proteins along a particular direction. This, of course, presupposes that the effects of cell-surface heterogeneity upon protein transport are of secondary importance compared to the effects of τ_c and K. The validity of this condition and the relevance of the correlation time scale τ_c are examined later through comparisons of model predictions with a reanalysis of existing SPT data of the major histocompatibility complex (MHC) in HeLa cells and fibroblasts.

Perhaps the simplest extension of Eq. (1) with the potential for encapsulating the peculiar transport characteristics of individual cell receptors arises when it is combined in a sequential manner with trapping events. The time elapsing between two successive jumps is drawn from a waiting time PDF $w(t)$. For times much longer than the characteristic waiting time (i.e., the average waiting time) $T=\int_0^\infty dt\, tw(t)$, the dynamics effectively revert back to that of free Brownian motion. It has yet to be established in experiment whether the anomalous diffusion characteristics of proteins show a crossover to normal diffusion at large times or is anomalous at all times [9]. If such a transition does exist then it must occur at a time exceeding the duration of the experiments. Consequently when considering the transport processes occurring during the duration of the experiments, the mean waiting time T can be taken to be a divergent quantity. Here, in the spirit of Nagle [17], who used a continuous time random walk model to examine the effects of long-time tails on fluorescence photobleaching recovery, we take $w(t) \sim \tau^\alpha / t^{1+\alpha}$, where $0<\alpha<1$ and τ is the intrinsic time scale of the waiting process. A power-law distribution of trapping times arise when, for example, the energies E_i governing the residence times $\exp(\beta E_i)$, within binding sites is exponentially distributed, $P(E)=\lambda e^{-\lambda E}$. Then the distribution of the waiting times is a power law of the form $P(t)dt = (t^{-(\lambda/\beta+1)} 2\lambda/\beta)dt$. In this immobilizing-release-walking scenario, the evolution of the PDF, $P(x,t)$, for the displacement x at time t of a Brownian particle is described by a fractional telegraph equation [18]

$$\frac{\partial P(x,t)}{\partial t} + \frac{\tau^\alpha}{2}\, {}_0D_t^{1+\alpha} P(x,t) = K\, {}_0D_t^{1-\alpha} \frac{\partial^2 P(x,t)}{\partial x^2}, \qquad (2)$$

where the Riemann-Liouville operator ${}_0D_t^{1-\alpha} = (\partial/\partial t)\, {}_0D_t^{-\alpha}$ is defined by

$${}_0D_t^{-\alpha} P(x,t) = \frac{1}{\Gamma(\alpha)} \int_0^t dt' \frac{P(x,t')}{(t-t')^{1-\alpha}} \qquad (3)$$

and $K_0 = k_B T/m\eta_\alpha$, where m is the mass of the Brownian particle, and η_α the friction coefficient. The Riemann-Liouville operator is a fractional integral of order α, and fractional derivatives may be established similarly via fractional integration and ordinary differentiation. At integer powers, the operator reduces to a standard integral. A detailed account of fractional calculus can be found in the book by Miller [19], and a good summary may be found in the Appendix of [20]. At short times $t<\tau^* = (mK/k_BT)\tau^{2\alpha-2}$, mean-square particle displacements from the origin evolve according to $\langle x^2\rangle = K_0 t^{2\alpha}/\tau\Gamma(2\alpha)$, whereas at much later times $t \gg \tau^*$ transport is subdiffusive, $\langle x^2\rangle = K_0 t^\alpha/\Gamma(\alpha)$, and non-Gaussian. Between these two asymptotes, the growth in the mean-square particle displacements changes continuously and smoothly. For an initial pointlike distribution of particles, the distribution of particle displacements at all later times t is given by a Fox function,

$$P(x,t) = \frac{1}{\sqrt{4\pi K t^\alpha}} H_{1,2}^{2,0}\left[\frac{x^2}{4Kt^\alpha} \middle| \begin{matrix} (1-\alpha/2,\alpha) \\ (0,1),(1/2,1) \end{matrix} \right] \qquad (4)$$

(for a definition of the H function see, for example, [20]). The flatness of this distribution

$$\frac{\langle x^4\rangle}{\langle x^2\rangle^2} = \frac{6\Gamma(1+\alpha)\Gamma(1+\alpha)}{\Gamma(1+2\alpha)} \qquad (5)$$

lies between 3 and 6 and consequently the distribution is broader than a Gaussian distribution which has a flatness of 3.

The situation changes somewhat when the correlation of the fluctuating force has a power-law time dependency $\langle F(0)F(t)\rangle = F_0(\beta)t^\beta$ where $0<\beta<2$. Such power-law correlations arise when particles are moving in a fluid with a density comparable to the particle itself or when a particle moves within a fluid having internal structure [21]. Both scenarios could form the basis for interpreting or modeling the motions of membrane-bound proteins. This power-law dependence of the correlation can either hinder the diffusive motion $(0<\beta<1)$, or enhance the diffusion $(1<\beta<2)$. The superdiffusive modes arise when successive fluctuations in the stochastic driving noise are positively correlated. The Fokker-Planck equation describing the evolution of particles subjected to fluctuating force with a power-law correlation is

$$ {}_0D_t^{1+\alpha} P(x,t) + \int_0^t \alpha_0(\beta)(t-\tau)^{-\beta} \frac{\partial P(x,\tau)}{\partial \tau} d\tau = K\, {}_0D_t^{1-\alpha} \frac{\partial^2 P(x,t)}{\partial x^2} \qquad (6)$$

[22]. For $0<\beta<1$, the second term on the left-hand side of Eq. (6) can be written as a Riemann-Liouville fractional derivative and so Eq. (6) can be rewritten as

$$\tau\, {}_0D_t^{1+\alpha} P(x,t) + {}_0D_t^{\beta} P(x,t) = K\, {}_0D_t^{1-\alpha} \frac{\partial^2 P(x,t)}{\partial x^2}. \qquad (7)$$

When ensemble averaged over realizations of the initial velocity, the mean particle displacements $\langle x\rangle = 0$. Mean-squared particle displacements from the origin evolve according to $\langle x^2\rangle \sim t^{2\alpha}$ at short times, while at long times $d\langle x^2\rangle/dt \sim t^{\alpha+\beta-2}$ and transport is either confined $(\alpha+\beta<1)$, subdiffusive $(1<\alpha+\beta<2)$, or superdiffusive $(\alpha+\beta>2)$. In the case of confined diffusion, the growth of the mean-squared particle displacements, rather than mean-squared particle dis-

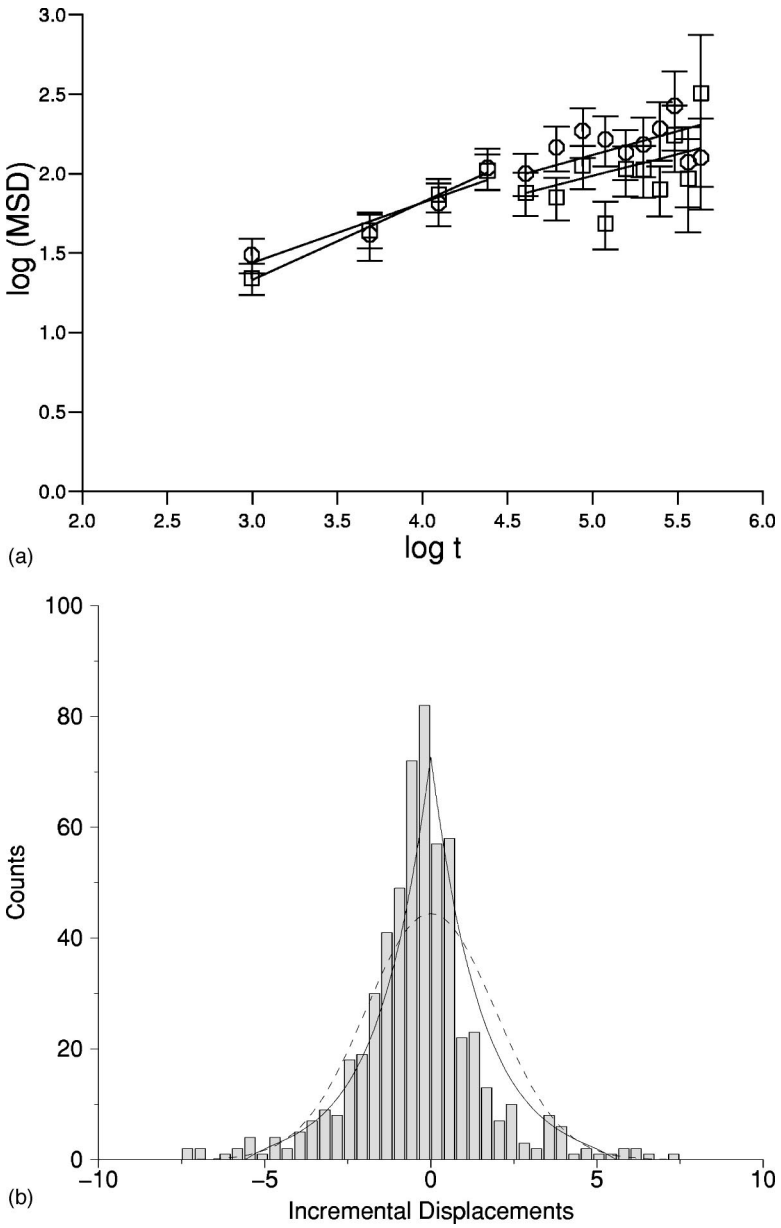

FIG. 1. (a) Ln-ln plot of the time evolution (in seconds) of the MSD (in pixels, using a scale of 0.205 μm/pixel) of MHC class II Fab-phycoerythrin on a fibroblast. Linear regression fits (dashed lines) to the short and long time behaviors are also shown. (b) Histogram of the incremental displacements in the x direction in pixels that occur within the 20 s intervals between successive observations. The ensemble is taken over the entire measurement time and over all trajectories within the data set. Gaussian (dotted line) and Fox function (solid line) PDFs with equivalent mean and variance are shown for comparison.

placements *per se*, vanishes at long times.

In the next section it is shown that the transport characteristics of cell receptors observed in single-particle tracking experiments are described accurately by the fractional telegraph equation Eq. (2) and its relative Eq. (7).

MEASUREMENT AND ANALYSIS OF SINGLE-PARTICLE TRACKING DATA

Single-particle fluorescence images were obtained using *R*-phycoerythrin as the fluorophore, conjugated to Fab fragments of antibodies against the human major histocompatibility complex. The labeled MHC class I antibody [8] was applied to HeLa cells, and the labeled antibody against MHC class II [23] was bound to fibroblasts transfected with the relevant MHC genes. Both these cell types provide flat areas of plasma membrane where small numbers (<500) of receptors are widely dispersed. The fluorophores can be detected by a cooled back-illuminated charge-coupled device camera, appearing as diffraction-limited spots; the exposure times were chosen to give signal-to-noise ratios greater than 4:1. Pixels in an area around the spot can be least-squares fitted by a two-dimensional Gaussian function [24] to determine the centroid position to a precision better than 40 nm in x and y. Linking these positions through images of a time series shows the track followed by the receptor in two dimensions. Global motion of the particles from microscope drift was determined by tracking off-cell spots that resulted from the probe adhering to the glass, and subtracted from the individual track positions; the mean distance moved over all tracks was an indicator of membrane motion (flow) and any cells showing this were not analyzed further. If the change of mean-square displacement with time interval is linear, a diffusion coefficient can be found from $\langle r^2 \rangle = 4D_l \delta t$. Analysis of immobile fluorescent particle tracks suggests the smallest observable value of D_l to be about 0.3×10^{-12} cm^2 s^{-1} [8].

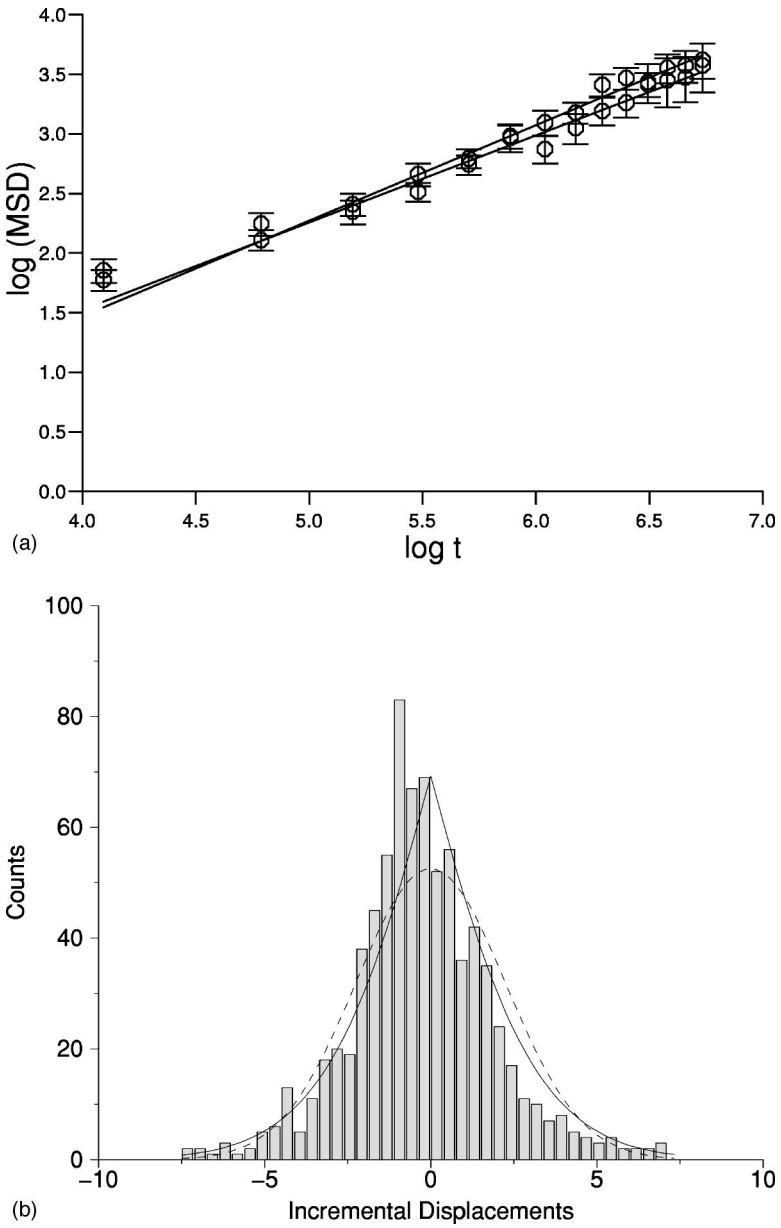

FIG. 2. (a) Ln-ln plot of the time-evolution (in seconds) of the MSD (in pixels, using a scale of 0.205 μm/pixel) of MHC class I. Linear regression fits (dashed lines) to the short and long time behaviors are also shown. (b) Histogram of the incremental displacements in the x direction in pixels that occur within the 60 s intervals between successive observations. The ensemble is taken over the entire measurement time and over all trajectories within the data set. Gaussian (dotted line) and Fox function (solid line) PDFs with equivalent mean and variance are shown for comparison.

COMPARISONS WITH DATA FROM SINGLE-PARTICLE TRACKING EXPERIMENTS

Single-particle tracking experiments can resolve movements of individual cell receptors with a precision down to 10 nm, depending on the probe used and the experimental conditions. There are, however, several limitations of the method which complicate data interpretation and model analysis. For example there may be a contribution to drag resulting from the interaction of the label with the extracellular matrix. In principle, at least, this could be accounted for by replacing the true mass m of a protein, which appears in Eq. (2) as a model parameter, with an effective mass m^*. Other complicating factors include the cross-link binding of sites by multivalent labels, which may result in a reduction of diffusivity and which trigger biological responses such as transmembrane signaling; and antibody binding which may affect the interactions between the labeled protein and other proteins. These complicating factors are incorporated into the model by replacing the actual distribution of waiting times (i.e., the value of α) with an effective distribution of waiting times which characterizes all the possible binding processes.

Photobleaching and trajectory interception limit the maximum number of data points for a receptor track to about 20. Following the approach of Anderson *et al.* [24], effects of statistical noise were reduced in determining mean-squared particle displacements (MSDs) in a time period t by averaging over all pairs of data points separated temporally by Δt rather than by averaging over particle displacements at time $t=\Delta t$ relative to their position at the origin of time. In Anderson *et al.* [24], only independent pairs of data points were used. The scatter is considerably greater when only independent pairs of data points are used, but the general behavior of the MSD is unchanged. Hence, to reduce the scatter, and hence the error in the exponents, nonindependent averaging has been used for calculation of exponents. To facilitate com-

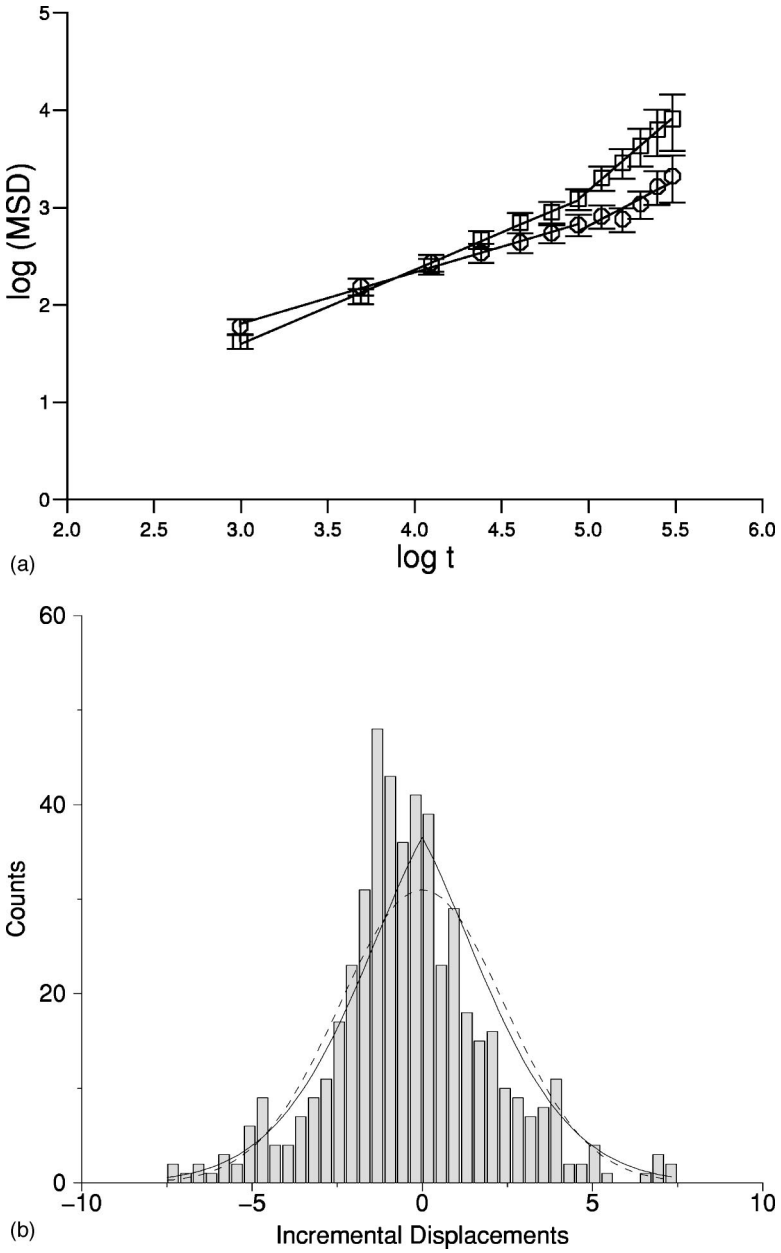

FIG. 3. (a) Ln-ln plot of the time evolution (in seconds) of the MSD (in pixels, using a scale of 0.205 μm/pixel) of MHC class II Fab-phycoerythrin on a fibroblast. Linear regression fits (dashed lines) to the short and long time behaviors are also shown. (b) Histogram of observed incremental displacements in the x direction in pixels that occur within the 20 s interval between successive observations. The ensemble is taken over the entire measurement time and over all trajectories within the data set. Gaussian (dotted line) and Fox function (solid line) PDFs with equivalent mean and variance are shown for comparison.

parisons with predictions from the one-dimensional model, it is assumed that components of the observed displacements of proteins can be treated independently. The distribution of incremental displacements in each direction was also recorded by considering all pairs of data points in the sample separated by a single time step.

Figure 1 shows an example of subdiffusion, a transition between modes of diffusive transport, and a non-Gaussian distribution of incremental displacements. The data were obtained from a reanalysis of previously acquired MHC class II Fab-phycoerythrin on a fibroblast at 20 °C [25]. The data set comprises 79 tracks, each with 15 data points acquired at 20 s intervals. Many earlier experiments on the MHC complex have indicated cell surface heterogeneity on spatial scales much smaller than the expected 20 s diffusion interval. The data capture the cumulative effects of these inhomogeneities. In accordance with model predictions there is a transition from a regime characterized by $\langle x^2\rangle \sim t^{2\alpha}$ to one where $\langle x^2\rangle \sim t^{\alpha}$. A linear regression fit with a transition occurring after four data points yields $\alpha = 0.25$. This estimate is comparable with the mean-squared independent $\alpha = 0.23$ obtained using Eq. (5) in conjunction with the long-time flatness statistic $\langle x^4\rangle / \langle x^2\rangle^2 = 5.63$ of the data. The observed distribution of incremental displacements in the x direction (i.e., displacements occurring within the 20 s interval between successive observations) is seen to be well represented by the predicted Fox function with $\alpha = 0.25$ when the variance is matched to the data. The distribution cannot be well represented by a Gaussian distribution of similar variance, further indicating that the diffusion present is not normal diffusion, but is strongly anomalous in character. In the y direction the transition is from a regime characterized by $\langle y^2\rangle \sim t^{0.38}$ to one where $\langle y^2\rangle \sim t^{0.13}$. The short length of the data set, and corresponding errors in finding the exponent by curve fitting,

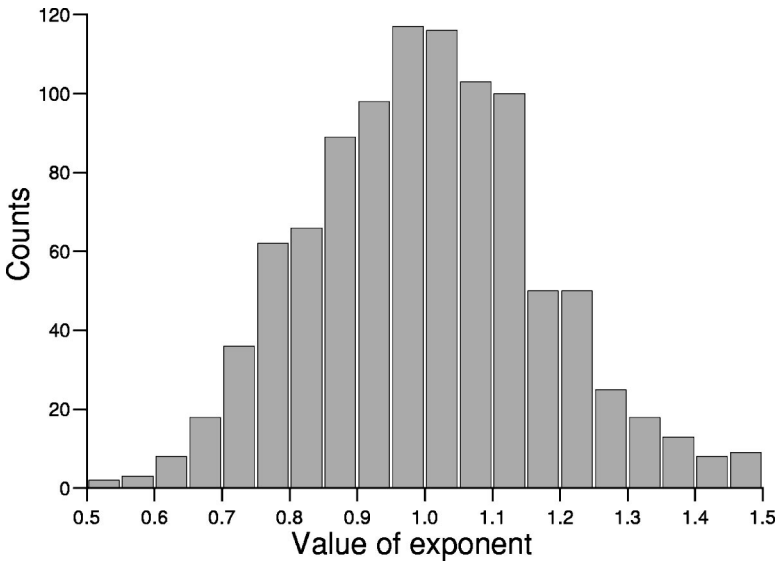

FIG. 4. Distribution of the diffusion exponents found when using simulated normal diffusion data.

are sufficient to explain the difference in exponent between the x and y directions. The long-time flatness statistic for the y direction of 6.43 indicates strongly anomalous diffusion, but Eq. (5) is not valid for values greater than 6, and hence it is not possible to calculate an anomalous diffusion exponent from the statistic in this case.

The correspondence between diffusion exponent α and distribution function finds further support in the reanalysis of data for MHC class 1 shown in Fig. 2 [8]. This data set comprises 72 tracks, each with 13 data points acquired at 60 s intervals. A linear regression fit to the MSD data yields $\langle x^2\rangle \sim t^{0.80}$, and in the y direction, $\langle y^2\rangle \sim t^{0.73}$. The slight difference in the exponents for the two directions can again be explained by the inaccuracies inherent in the method. The absence of a transition in the evolution of the mean-squared displacements may indicate that the transition time is shorter than the sampling interval or longer than the duration of the records. For example in the x direction, in the former case $\alpha=0.80$ while in the latter case $2\alpha=0.80$. The flatness statistic for the x direction of this data set of 3.50 gives an estimate for α of 0.84, indicating the first of these two cases. In the y direction the flatness statistic of 4.54 indicates an anomalous diffusion exponent of 0.55. Figure 2 shows that the distribution of incremental displacements in the x direction is well represented by a Fox function with $\alpha=0.80$ when the variance is matched to the data.

Shown in Fig. 3 is an example of a transition from sub- to superdiffusive transport. As in a previous example, the data were obtained from a reanalysis of acquired data for MHC class II Fab-phycoerythrin on a fibroblast at 20 °C. The data set comprises 81 tracks, each with 14 data points acquired at 20 s intervals. There is no evidence of a mean drift in any particular direction, and hence there is no directed motion present. Linear regression fits to the MSD data yields $\langle x^2\rangle \sim t^{0.76}$ at short times and $\langle x^2\rangle \sim t^{1.54}$ at long times, whereas in the y direction the transition is from $\langle y^2\rangle \sim t^{0.53}$ to $\langle y^2\rangle \sim t^{0.99}$. Both these results are compatible with model predictions, $\langle x^2\rangle \sim t^{2\alpha}$ and $\langle x^2\rangle \sim t^{\alpha+\beta-1}$, for the case of power-law correlated noise if $\alpha_x=0.38$, $\alpha_y=0.27$, $\beta_x=1.92$, and $\beta_y=1.72$. The difference between β_x and β_y is not statistically significant. It is evident from Fig. 3 that the distribution of incremental displacements in the x direction is well approximated by a Fox function probability density function with parameter 0.76. Evidence for superdiffusion (by the Levy flight mechanism) has previously been reported in a photobleaching study of the diffusion of dye bound to cylindrical micelles [26].

As a control, a similar analysis was performed on a set of simulated normal diffusion trajectories with the same sample size as the smallest of the samples presented here. Data were simulated using a simple random walk model with Gaussian jumps occurring at constant time intervals. The distribution of exponents found is shown in Fig. 4, and are seen to fall mainly near 1, but with some scatter due to the smallness of the data set. No transitions were seen, and distributions of incremental displacements were close to Gaussian. Thus it is clear that these results are not an artifact of the method of analysis used.

CONCLUSIONS

It has been shown that the transport characteristics of individual cell receptors observed in SPT can be understood in terms of the imposition of immobilizing events onto Brownian motion. The immobilizing events model phenomologically obstruction by mobile or immobile proteins, transient binding to immobile proteins, confinement of skeletal corrals, binding to the extracellular matrix and restrictions to motions imposed by lipid domains. The transition from $\langle x^2\rangle \sim t^{2\alpha}$ to $\langle x^2\rangle \sim t^{\alpha}$ growth of mean-square displacements and the Fox distributions of incremental displacements predicted by this model were shown to be well supported by a reanalysis of previously acquired data for MHC class I and II Fab-phycoerythrin on a fibroblast.

Monte Carlo simulations have provided evidence of a

crossover from anomalous to normal diffusion at long times [27]. Establishing whether the anomalous diffusion characteristics of proteins actually show a crossover to normal diffusion at large times or remain anomalous at all times remains a key issue to be resolved.

ACKNOWLEDGMENTS

This work was funded by the BBSRC and the EPSRC through Grant No. 204/E17847. We thank Pheobe Lynn for assistance with the data analysis.

[1] R. N. Ghosh and W. W. Webb, Biophys. J. **53**, A352 (1988).
[2] R. N. Ghosh and W. W. Webb, Biophys. J. **57**, A286 (1990).
[3] R. N. Ghosh and W. W. Webb, Biophys. J. **66**, 1301 (1994).
[4] A. Kusumi, Y. Sako, and M. Yamamoto, Biophys. J. **65**, 2021 (1993).
[5] M. Edidin, J. Cell Sci. Suppl. **17**, 165 (1993).
[6] J. P. Slattery, Ph.D. thesis, Cornell University, Ithaca, NY, 1995.
[7] T. J. Feder, I. Brust-Mascher, J. P. Slattery, B. Baird, and W. W. Webb, Biophys. J. **70**, 2767 (1996).
[8] P. R. Smith, I. E. G. Morrison, K. M. Wilson, N. Fernandez, and R. J. Cherry, Biophys. J. **76**, 3331 (1999).
[9] M. J. Saxton and K. Jacobson, Annu. Rev. Biophys. Biomol. Struct. **26**, 373 (1997).
[10] M. Kopf, C. Corinth, O. Haferkamp, and T. F. Nonnenmacher, Biophys. J. **70**, 2950 (1996).
[11] C. E. Schmidt, T. Chen, and D. A. Lauffenburger, Biophys. J. **67**, 461 (1994).
[12] M. P. Sheetz, S. Turney, H. Qian, and E. L. Elson, Nature (London) **340**, 284 (1989).
[13] M. P. Sheetz and S. C. Kuo, Methods Cell Biol. **39**, 129 (1993).
[14] S. Chandrasekhar, Rev. Mod. Phys. **15**, 1 (1943).
[15] W. L. C. Vaz and P. F. Almeida, Biophys. J. **60**, 1553 (1991).
[16] J. H. Freed, Annu. Rev. Biophys. Biomol. Struct. **23**, 1 (1994).
[17] J. F. Nagle, Biophys. J. **63**, 336 (1992).
[18] R. Metzler and J. Klafter, J. Phys. Chem. B **104**, 3851 (2000).
[19] K. S. Miller and B. Ross, *An Introduction to the Fractional Calculus and Fractional Differential Equations* (Wiley, New York, 1993).
[20] R. Metzler and J. Klafter, Phys. Rep. **339**, 1 (2000).
[21] K. G. Wang, Phys. Rev. A **45**, 833 (1992).
[22] S. Khan and A. M. Reynolds, Physica A **350**, 183 (2005).
[23] K. M. Wilson, I. E. G. Morrison, P. R. Smith, N. Fernandez, and R. J. Cherry, J. Cell. Sci. **109**, 2101 (1996).
[24] C. M. Anderson, G. N. Georgiou, I. E. G. Morrison, G. V. W. Stevenson, and R. J. Cherry, J. Cell. Sci. **101**, 415 (1992).
[25] S. Mushtaq, M.Sc. thesis, University of Essex, 1999.
[26] A. Ott, J. P. Bouchard, D. Langevin, and W. Urbach, Phys. Rev. Lett. **65**, 2201 (1990).
[27] M. J. Saxton, Biophys. J. **70**, A311 (1996).